

<http://mc.manuscriptcentral.com/fems>

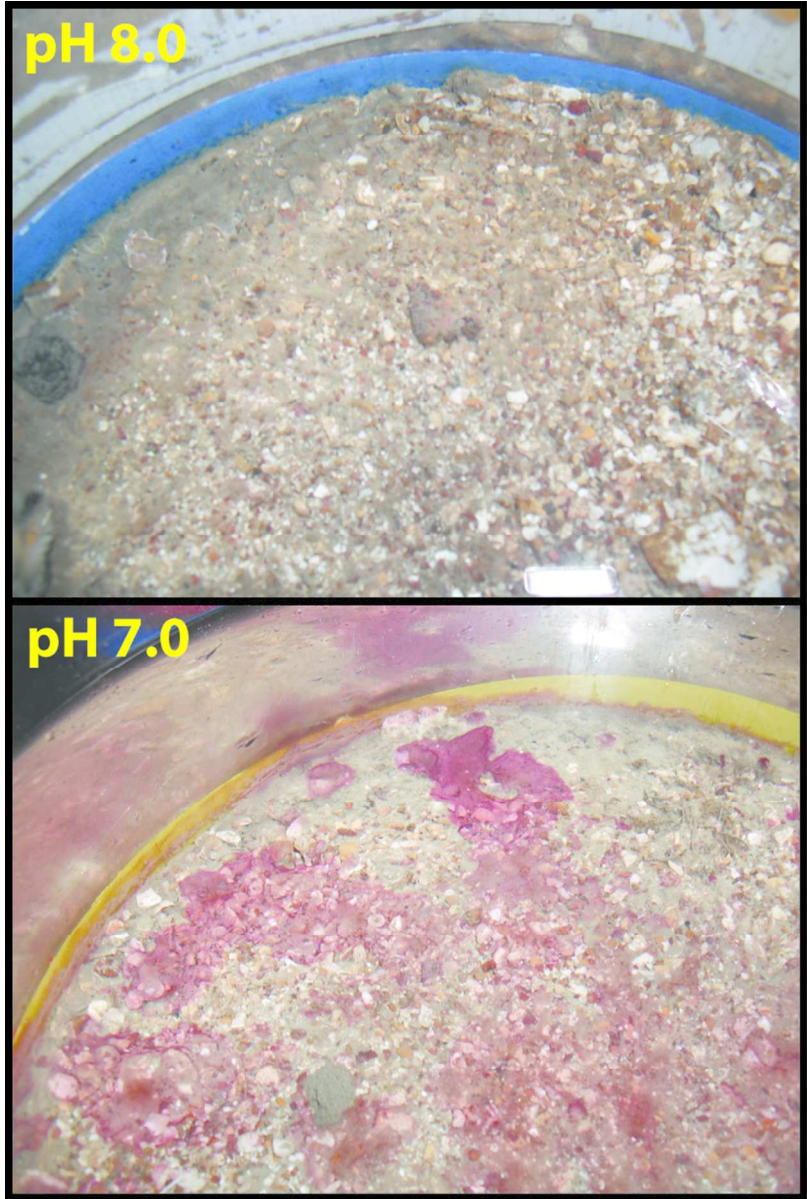
## Elevated CO<sub>2</sub> induces a bloom of microphytobenthos within a shell gravel mesocosm

Journal:	<i>FEMS Microbiology Ecology</i>
Manuscript ID:	FEMSEC-14-12-0663.R1
Manuscript Type:	Research Paper
Date Submitted by the Author:	n/a
Complete List of Authors:	Tait, Karen; Plymouth Marine Laboratory, MLSS Beesley, Amanda; Plymouth Marine Laboratory, MLSS Findlay, Helen; Plymouth Marine Laboratory, MLSS McNeill, Caroline; Plymouth Marine Laboratory, MLSS Widdicombe, Stephen; Plymouth Marine Laboratory, MLSS
Keywords:	Carbon Dioxide Capture and Storage, Sediment, Microphytobenthos, 16S rRNA 454 pyrosequencing, quantitative PCR

SCHOLARONE™  
Manuscripts

Review

1  
2  
3  
4  
5  
6  
7  
8  
9  
10  
11  
12  
13  
14  
15  
16  
17  
18  
19  
20  
21  
22  
23  
24  
25  
26  
27  
28  
29  
30  
31  
32  
33  
34  
35  
36  
37  
38  
39  
40  
41  
42  
43  
44  
45  
46  
47  
48  
49  
50  
51  
52  
53  
54  
55  
56  
57  
58  
59  
60



A transient bloom of the cyanobacteria *Spirulina* sp. together with associated diatoms formed on the surface of sediments exposed to CO<sub>2</sub>-acidified seawater at pH 7.5 and 7.0, but not at pH 8.0.  
69x103mm (300 x 300 DPI)

1  
2  
3 **1 Elevated CO<sub>2</sub> induces a bloom of microphytobenthos within a shell gravel mesocosm**  
4

5 2

6 3 Karen Tait\*, Amanda Beesley, Helen S. Findlay, C. Louise McNeill, Stephen Widdicombe  
7

8 4 Plymouth Marine Laboratory, Prospect Place, Plymouth, PL1 3DH, UK  
9

10 5

11 6 Corresponding Author: Karen Tait, Plymouth Marine Laboratory, Prospect Place, Plymouth, PL1 3DH.  
12

13 7 Tel: +44 1752 633415; Fax: +44 1752 633101; ktait@pml.ac.uk  
14

15 8

16 9 Running title: Elevated CO<sub>2</sub> induces microphytoplankton bloom  
17

18 10

19 11 Key words: CCS, microphytobenthos, sediment, 16S rRNA 454 pyrosequencing, quantitative PCR,  
20

21 12 nutrient fluxes  
22  
23  
24  
25  
26  
27  
28  
29  
30  
31  
32  
33  
34  
35  
36  
37  
38  
39  
40  
41  
42  
43  
44  
45  
46  
47  
48  
49  
50  
51  
52  
53  
54  
55  
56  
57  
58  
59  
60

**Abstract**

The geological storage of carbon dioxide (CO<sub>2</sub>) is expected to be an important component of future global carbon emission mitigation, but there is a need to understand the impacts of a CO<sub>2</sub> leak on the marine environment and to develop monitoring protocols for leakage detection. In the present study, sediment cores were exposed to CO<sub>2</sub>-acidified seawater at one of five pH levels (8.0, 7.5, 7.0, 6.5 and 6.0) for 10 weeks. A bloom of *Spirulina* sp. and diatoms appeared on sediment surface exposed to pH 7.0 and 7.5 seawater. Quantitative PCR measurements of the abundance of 16S rRNA also indicated an increase to the abundance of microbial 16S rRNA within the pH 7.0 and 7.5 treatments after 10 weeks incubation. More detailed analysis of the microbial communities from the pH 7.0, 7.5 and 8.0 treatments confirmed an increase in the relative abundance of *Spirulina* sp. and *Navicula* sp. sequences, with changes to the relative abundance of major archaeal and bacterial groups also detected within the pH 7.0 treatment. A decreased flux of silicate from the sediment at this pH was also detected. Monitoring for blooms of microphytobenthos may prove useful as an indicator of CO<sub>2</sub> leakage within coastal areas.

**Introduction**

Increasing political, social and environmental pressure to alleviate future impacts from global warming and ocean acidification has led many countries to commit to reducing their carbon emissions. One potential mitigation strategy is Carbon Capture and Storage (CCS). This involves the capturing of waste CO<sub>2</sub> from large industries such as coal and natural gas fired power plants, transporting it to a storage site and depositing it underground in geological formations such as depleted oil and gas fields, unmineable coal seams or deep saline formations. CCS technology has the potential to reduce CO<sub>2</sub> emissions from fossil fuel power stations by 80–90% (Holloway, 2007) and the Intergovernmental Panel on Climate Change (IPCC) recognises that effective CCS could play a substantial role in mitigation, potentially reducing CO<sub>2</sub> emissions overall by 21 – 45 % by 2050 (Metz et al, 2005). The development and deployment of technology required for CO<sub>2</sub> capture, transport and storage are making the application of CCS to reduce CO<sub>2</sub> emissions more feasible. Industrial-scale CCS projects are now in operation in Algeria, Norway, Canada and the USA, with many more demonstration and pilot scale ventures in construction globally. The majority of these are on-shore, storing CO<sub>2</sub> within deep saline formations, coal seams and gas fields (Global CCS Institute, 2012). However, many potential projects are considering off-shore storage, including schemes in Australia, Korea, China, and Italy with several projects aiming to store CO<sub>2</sub> in deep saline formations or abandoned oil and gas fields in the North Sea, including the Netherlands ROAD project, Norway's

1  
2  
3 47 Mongstad project and the pilot-level projects in the UK (Global CCS Institute, 2012). Currently, at the  
4 48 Sleipner site in the North Sea, CO<sub>2</sub> from produced gas is directly captured and stored in a subsea  
5 49 aquifer and the Norwegian project Snøhvit, a petroleum production plant in the Barents Sea, is  
6 50 currently capturing CO<sub>2</sub> at their on-shore site and storing off-shore.  
7  
8  
9

10 51  
11 52 Although leakage from storage sites is considered to be unlikely, leakage back up the injection pipe  
12 53 is considered to be a greater risk. If CO<sub>2</sub> leakage did occur from geological storage or pipeline failure,  
13 54 it has the potential to create considerable localised reductions in seawater pH (Blackford et al. 2008;  
14 55 2009; 2014). Elevated levels of CO<sub>2</sub> can be detrimental to some marine microbes that rely on  
15 56 carbonate structures (Langer et al. 2009; Beaufort et al. 2011), and can also impact microbially-  
16 57 driven biogeochemical nutrient cycling (Hutchins et al. 2007; Fu et al. 2008; Beman et al. 2011;  
17 58 Kitidis et al., 2011). However, only a small number of studies have considered microbial communities  
18 59 and processes within sediments (Ishida et al. 2005; Håvelsrud et al. 2012; Håvelsrud et al. 2013;  
19 60 Ishida et al. 2013; Tait et al., 2013; Tait et al. 2015; Yanagawa et al. 2013; Kerfahi et al. 2014). These  
20 61 studies have reported decreases in microbial diversity (Yanagawa et al. 2013; Kerfahi et al. 2014; Tait  
21 62 et al. 2015), increases to the abundance of bacteria and archaea (Ishida et al. 2005; Ishida et al.  
22 63 2013), and also possible changes to the degradation of organic matter and biogeochemical cycling of  
23 64 nutrients, including enhanced methane production and sulphate reduction (Ishida et al. 2013;  
24 65 Yanagawa et al. 2013).  
25  
26  
27  
28  
29  
30  
31  
32  
33  
34

35 67 Due to their rapid response to environmental changes, a change to microbial activity or community  
36 68 composition could provide an indication of increased pCO<sub>2</sub> or lowered pH. A recent CO<sub>2</sub> release  
37 69 experiment that occurred in the field in Ardmucknish Bay (Oban, Scotland) highlighted the possibility  
38 70 of using microbes and microbial activity as an indicator of CO<sub>2</sub> leaks (Tait et al. 2015). In this  
39 71 instance, a borehole was drilled from shore through the bedrock and into unconsolidated sediments  
40 72 at a location 350 m offshore, and CO<sub>2</sub> gas supplied through a stainless steel pipeline with a gas  
41 73 diffuser welded to the end (11 m below the seabed, which was in turn 12 m below mean sea-level)  
42 74 (Taylor et al. 2015a). A total of 4.2 tonnes of CO<sub>2</sub> were injected into the overlying unconsolidated  
43 75 sediments, but the majority of CO<sub>2</sub> injected *via* the sub-seabed pipe was retained within the  
44 76 sediments. Only ~15 % of the total CO<sub>2</sub> injected was estimated to have been emitted from the  
45 77 seabed in a gaseous phase (Blackford et al. 2014). Bubbles of CO<sub>2</sub> were clearly visible entering the  
46 78 water column and **these dissolved rapidly**, with measurements of pCO<sub>2</sub> in bottom water at the  
47 79 injection site **ranging from** 380 to 1500 µatm, depending on injection rate and tidal state  
48 80 (Atamanchuck et al. 2014) and pH measurements within the surface sediments dropped by 0.85 pH  
49  
50  
51  
52  
53  
54  
55  
56  
57  
58  
59  
60

1  
2  
3 81 units (Taylor et al. 2015b). Benthic microbes were shown to respond rapidly to the sub-seabed  
4 82 release of CO<sub>2</sub>: increases in the abundance of microbial 16S rRNA g<sup>-1</sup> sediment, used as a proxy for  
5 83 microbial activity, could be detected within the area of active bubble leakage after 14 days of CO<sub>2</sub>  
6 84 release (Tait et al. 2015). There was also evidence that the high CO<sub>2</sub> plume in the water column was  
7 85 advected to a distance of 25 m due to tidal circulation (Atamanchuk et al. 2015), and changes to the  
8 86 abundance of 16S rRNA were also detected at this distance, suggesting that microbes may be highly  
9 87 sensitive to a sub-seabed CO<sub>2</sub> leak. Terminal Restriction Fragment Length Polymorphism (T-RFLP)  
10 88 analysis of the active bacterial community also indicated a rapid shift in composition within areas  
11 89 impacted by the CO<sub>2</sub> release (Blackford et al. 2014). Also evident was a decrease in the abundance  
12 90 of microbial 16S rRNA genes at the leak epicentre during the initial recovery phase that coincided  
13 91 with the highest measurements of DIC within the sediment, but may also be related to the release of  
14 92 potentially toxic metals at this time point (Lichtschalg et al. 2014).  
15  
16  
17  
18  
19  
20  
21  
22  
23

24 94 The controlled CO<sub>2</sub> release experiment in Ardmucknish Bay clearly showed that detection of changes  
25 95 to pH or CO<sub>2</sub> may be challenging. Despite the high levels of CO<sub>2</sub> released during the later stages of  
26 96 CO<sub>2</sub> release at the QICS site, pH actually increased as the rise in DIC was buffered by the dissolution  
27 97 of sediment calcium carbonate (Blackford et al. 2014). Different strategies for monitoring potential  
28 98 CO<sub>2</sub> leaks are, therefore, required. The QICS study identified possible microbial indicators for CO<sub>2</sub>  
29 99 leakage within coastal environments; this included an increase in the activity of *Cyanobacteria* and  
30 100 micro-algae, or microphytobenthos during the highest CO<sub>2</sub> release period. Microphytobenthos can  
31 101 be found in the photic zone of marine environments and are composed of microalgae,  
32 102 predominantly *Baccillariophyceae*, but *Chlorophyceae* and *Dinophyceae* can also be present, and  
33 103 bacteria including *Cyanobacteria*, heterotrophic bacteria, chemolithotrophic bacteria, anoxygenic  
34 104 phototrophs and sulphate-reducing bacteria (Paterson & Hagerthey, 2001; Hubas et al. 2011). These  
35 105 microbes accumulate at the sediment surface and exhibit high rates of photosynthesis, contributing  
36 106 up to 50% of estuarine primary production (Underwood and Kromkamp, 1999), and fuelling much of  
37 107 the secondary production within these ecosystems (Middleburg et al, 2000).  
38  
39  
40  
41  
42  
43  
44  
45  
46  
47  
48

49 109 In the present study, fifty cores containing carbonate rich gravel collected from the Eddystone reef  
50 110 in the Western English Channel (50° 11.55 N, 04° 17.0 W) during September 2010 were incubated  
51 111 using seawater adjusted to five different CO<sub>2</sub> concentrations by bubbling with pure CO<sub>2</sub>, the flow of  
52 112 which was monitored *via* an electronic feedback system. Twenty five sediment cores were incubated  
53 113 for a period of 2 weeks and the remainder for 10 weeks. The aim of the experiment was to examine  
54 114 the impact of a CO<sub>2</sub> leak on meio- and macrofauna residing within the sediments. However, during  
55  
56  
57  
58  
59  
60

1  
2  
3 115 the course of the experiment, a pink microphytobenthos mat appeared on top of the cores exposed  
4 116 to seawater adjusted to pH 7.0 and 7.5, providing the opportunity to identify key microbial species  
5 117 responding to elevated CO<sub>2</sub> levels. Surface sediment samples were taken for microbial analyses, the  
6 118 *Cyanobacteria* and micro-algae resident within the mat were identified, and the abundance of  
7 119 *Cyanobacteria* and micro-algae within the different pH treatments compared at two and ten weeks.  
8 120 This was followed by a detailed analysis of the microbial community present at week ten in cores  
9 121 receiving ambient pH seawater, and seawater adjusted to pH 7.0 and 7.5. After a two and ten week  
10 122 incubation period, measurements were made of the flux of nutrients from the sediment to the water  
11 123 column.  
12 124  
13 125

## 126 **Materials and Methods**

### 127 *Mesocosm set-up*

128 Carbonate rich gravel was collected on the 15<sup>th</sup> September 2010 from the Eddystone reef in the  
129 Western English Channel (50° 11.55 N, 04° 17.0 W). Sediment was collected using a 0.1 m<sup>2</sup> boxcorer  
130 and used to fill 50 clear Perspex cores (19 cm diameter, 40 cm deep) to a depth of 30 cm and topped  
131 off with seawater (10 cm depth) to prevent desiccation and minimise temperature change. Cores  
132 were transferred to the seawater acidification facility located in the mesocosm of the Plymouth  
133 Marine Laboratory (PML), UK. Once at PML the cores were continuously supplied with natural  
134 seawater collected from the Eddystone reef site (temperature ≈11 °C, salinity ≈ 34) at a rate of 15  
135 mL min<sup>-1</sup> for a period of 6 days to allow both the fauna and biogeochemical profiles within the cores  
136 to recover.  
137

138 The Ardmucknish Bay experiments indicated the CO<sub>2</sub> was emitted from the sediment as gas bubbles  
139 that rapidly dissolved, reducing the pH in the sediment/water boundary layer (Taylor et al. 2015b).  
140 Within this experiment, the 50 cores were randomly allocated to 1 of 5 pH treatment levels (8.0  
141 [control], 7.5, 7.0, 6.5 and 6.0) and supplied with unfiltered seawater from one of five header tanks  
142 at a rate of approximately 15 mL min<sup>-1</sup>. Seawater for the header tanks was collected from the  
143 Western English Channel Observatory long term monitoring site L4 (50° 15.00' N, 4° 13.02' W). The  
144 seawater in each of the pH 7.5, 7.0, 6.5 and 6.0 header tanks was maintained at the desired pH by  
145 bubbling with pure CO<sub>2</sub>, following the methodology of Widdicombe and Needham (2007). No  
146 additional CO<sub>2</sub> was added to the pH 8.0 tank. The temperature within the mesocosm was  
147 maintained at 11 °C, with a light: dark cycle of 16 h: 8 h. The water within each of the reservoir tanks  
148 and sediment cores was monitored three times per week for temperature, salinity (WTW LF187

1  
2  
3 149 combination temperature and salinity probe), and pH (Metrohm, 826 pH mobile with a Metrohm  
4 150 glass electrode, calibrated to NBS). Water samples were taken once a week to determine total  
5 151 alkalinity (TA) and nutrient concentrations. Nutrients were analysed with an autoanalyser (Brann &  
6 152 Luebbe Ltd., AAIII) using standard methods (Brewer & Riley, 1965; Grasshoff, 1976; Kirkwood, 1989;  
7 153 Mantoura & Woodward, 1983; Zhang & Chi, 2002). Alkalinity was measured by poisoning 100 mL  
8 154 water samples with HgCl<sub>2</sub> according to Dickson et al. (2007) then analysing via potentiometric  
9 155 titration using an Alkalinity Titrator (Apollo SciTech Model AS-ALK2) and using Batch 100 certified  
10 156 reference materials from Andrew Dickson. Using pH, TA, temperature, salinity, phosphate and  
11 157 silicate, the other carbonate parameters (dissolved inorganic carbon (DIC), pCO<sub>2</sub>, calcite and  
12 158 aragonite saturation states, etc.) were calculated using the CO2SYS programme (Pierrot et al. 2006)  
13 159 using constants from Mehrbach et al. (1973) refitted by Dickson and Millero (1987) and the KSO<sub>4</sub>  
14 160 dissociation constant from Dickson (1990).

15 161  
16 162 Two weeks after the start of the exposure (5th – 6th October 2011), five cores from each pH  
17 163 treatment (25 cores in total) were randomly selected and sampled for measurements of sediment  
18 164 nutrient flux, microbial abundance and community structure (described below) and then  
19 165 destructively sampled for meiofauna and macrofauna analysis (to be reported elsewhere). The  
20 166 remaining 25 cores were allowed to run for an additional 8 weeks before being similarly sampled  
21 167 (29th – 30th November 2011).

#### 22 168 23 169 *Sediment nutrient flux*

24 170 From each core, water samples were taken from the overlying 10 cm of water to determine the rate  
25 171 of sediment flux for five nutrient species (nitrate, nitrite, ammonium, silicate and phosphate). Over  
26 172 two consecutive days, three 50mL water samples were drawn from each core, filtered through a  
27 173 47mm ø GF/F filter into an acid washed Nalgene bottle and immediately frozen. In addition to these  
28 174 “core water” samples, five “inflow water” samples were taken from each of the five header tanks.  
29 175 These samples were also filtered and then frozen and analysed as described above for nutrient  
30 176 monitoring. Sediment fluxes were calculated using the equation:

$$31 177 F_x = \left( \frac{C_i - C_o}{A} \right) \cdot Q \quad (\text{Eq. 1})$$

32 178 where  $F_x$  is the flux of nutrient  $x$  ( $\mu\text{mol m}^{-2} \text{h}^{-1}$ ),  $C_i$  is the mean concentration of nutrient  $x$  in the  
33 179 inflow water ( $\mu\text{M}$ ),  $C_o$  is the mean concentration of nutrient  $x$  in the water above the sediment in the  
34 180 experiment cores ( $\mu\text{M}$ ),  $Q$  is the rate of water flow through the core ( $\text{L h}^{-1}$ ) and  $A$  is the area of the  
35 181 core ( $\text{m}^2$ ) (Widdicombe and Needham, 2007).

36 182

1  
2  
3 183 *Identification of Cyanobacteria and micro-algae community within the pink microphytobenthos mat*  
4  
5 184 During week 6, small sections of the pink microphytobenthos mat were removed from the surface of  
6  
7 185 the pH 7.0 and 7.5 cores at week 7 with a sterile scalpel and washed gently with filter-sterilised pH  
8  
9 186 7.0 or pH 7.5 seawater to remove sediment material. A light microscope (Reichert Jung Polyvar) and  
10  
11 187 an Optronics Magna Fire SP camera was used to image small sections of the material. DNA was  
12  
13 188 extracted from six small sections (0.2g) of the pink mat using the PowerBiofilm™ DNA Isolation Kit  
14  
15 189 (MoBio Laboratories) according to the manufacturer's instructions. To taxonomically identify the  
16  
17 190 cyanobacteria and algae present within the pink mat, PCR amplification of 16S rRNA gene fragments  
18  
19 191 was performed using the PCR primer pair CYA-359F (5' GGGGAATYTTCCGCAATGGG-3') and CYA-  
20  
21 192 781R (5'-GACTACWGGGGTATCTAATCCCW-3'), which are specific for Cyanobacteria and micro-algae  
22  
23 193 chloroplast (Nübel et al., 1997), using the PCR conditions described in Tait et al. (2015). This was  
24  
25 194 done in triplicate for each of the six DNA extractions and the PCR products cloned and transformed  
26  
27 195 using the pGEM-T Easy Vector System II cloning kit (Promega) according to the manufacturer's  
28  
29 196 instructions. Clone libraries were also made from DNA extracts of the day 0 samples to determine  
30  
31 197 the initial composition of the microphytobenthos community. Sequences were clustered into  
32  
33 198 Operational Taxonomic Units (OTUs) based on 97 % sequence similarity using Uclust (using the  
34  
35 199 QIIME (Quantitative Insights into Molecular Ecology ) pipeline; Caporaso et al. 2010). To assign  
36  
37 200 taxonomy to each OTU, a representative sequence from each OTU cluster was chosen, the  
38  
39 201 representative sequences aligned using PYNAST, and taxonomy assigned by comparison with the  
40  
41 202 Greengenes (version Feb 2011) (Pruesse et al. 2007) and the NCBI databases.

#### 203 204 *RNA extraction from sediments*

205 After 2 and 10 weeks incubation, 8 small sediment samples (approx. 0.5 g each) were taken from  
206 across the sediment surface (top 0.5 cm) in order to determine the composition of the active  
207 microbial community. The eight samples from each core were combined and homogenised, placed  
208 into 50 mL Falcon tubes, mixed with a sterile spatula and immediately frozen (-80 °C). This was  
209 compared to samples taken in a similar manner at the start of the experiment (day 0). RNA was  
210 extracted from 2 g of sediment using the MoBio RNA Powersoil Total RNA Isolation Kit (MoBio  
211 Laboratories) according to the manufacturer's instructions.

#### 212 213 *cDNA synthesis and RT-qPCR*

214 The RNA was reverse transcribed using the QuantiTect Reverse Transcription Kit (Qiagen) with 1 µL  
215 of RNA and the supplied random primers. An ABI 7000 sequence detection system (Applied  
216 Biosystems, Foster City, USA) and QuantiFast SYBR Green PCR Kit (Qiagen) was used for all qPCR

1  
2  
3 217 measurements. For each sediment sample, 1  $\mu$ L of cDNA was used to determine the abundance of  
4 218 cyanobacterial 16S rRNA using CYA359F and CYA781R and bacterial 16S rRNA using Bact1369F  
5 219 (CGGTGAATACGTTTCYCGG) and Prok1492R (GGWTACCTTGTTACGACTT) (Suzuki et al. 2000) following  
6 220 the methodology described in Tait et al. (2015). The 20  $\mu$ L reaction mixture contained 10  $\mu$ L of  
7 221 Master Mix and 300 nM of each primer, and PCR conditions were 5 min at 95  $^{\circ}$ C followed by 40  
8 222 cycles of 95  $^{\circ}$ C for 15 s, 52  $^{\circ}$ C for 30 s and 72  $^{\circ}$ C for 45 s. Standard curves were produced from cDNA  
9 223 following prior *in vitro* transcription of cloned sequences using the Ampliscribe T7 Flash kit  
10 224 (Epicentre) following methodologies described by Smith et al. (2006). 16S rRNA abundance was  
11 225 quantified via comparison to standard curves using the ABI Prism 7000 detection software.  
12 226 Automatic analysis settings were used to determine the threshold cycle (CT) values and baselines  
13 227 settings. The no-template controls were below the threshold in all experiments. For each standard  
14 228 curve, the slope, y intercept, co-efficient of determination ( $r^2$ ) and the efficiency of amplification was  
15 229 determined as follows: **Cyanobacteria**/chloroplast 16S rRNA:  $r^2 = 0.993$ , y intercept = 36.48,  $E = 94.5$   
16 230 %; bacterial 16S rRNA  $r^2 = 0.997$ , y intercept = 35.05,  $E = 96.3$  %.

17 231

#### 18 232 *16S rRNA 454 pyrosequencing and analysis*

19 233 An opportunity arose to have a small number of the sediment core samples analysed using 16S rRNA  
20 234 tagged 454 pyrosequencing. Twelve **cDNA samples (see above)** were chosen: 4 replicate cores from  
21 235 the pH 8.0, pH 7.5 and pH 7.0 treatments. These pH treatments were selected because of the  
22 236 presence of the pink mat, but also because the data would also be useful for studies of the impact of  
23 237 ocean acidification on sediment microbial communities. Possible changes to both bacterial and  
24 238 archaeal community composition was examined. For bacteria, cDNA was amplified with the V4-V5  
25 239 region of 16S rRNA using the PCR primers 518F (equal quantities of CCAGCAGCCGCGGTAAN and  
26 240 CCAGCAGCTGCGGTAAN) and 926R (equal quantities of CCGTCAATTCNTTTRAGT,  
27 241 CCGTCAATTCTTTGAGT and CCGTCAATTTCTTTGAGT) (Huse et al. 2010). For archaea, the PCR  
28 242 primers Parch519F (CAGCCGCCGCGGTAA) and ARC915R (GTGCTCCCCGCCAATTCCT) (Coolen et al.  
29 243 2004) were used. The 30  $\mu$ L-volume reaction mixtures contained 1  $\mu$ L of cDNA, 5X PCR buffer  
30 244 (Promega), 2.5 mM  $MgCl_2$ , 0.1 mM dNTPs, 1.5 U of GoTaq Hot Start DNA polymerase (Promega) and  
31 245 0.6  $\mu$ M of forward and reverse primers. PCRs were initially denatured for 3 mins at 94  $^{\circ}$ C, followed  
32 246 by 20 cycles of 94  $^{\circ}$ C for 30 secs; primer annealing at 57  $^{\circ}$ C for 45 secs, and elongation at 72  $^{\circ}$ C for 60  
33 247 secs. A final elongation step was performed at 72  $^{\circ}$ C for 5 min. A final 5 cycles were performed in a  
34 248 subsequent PCR reaction containing 1  $\mu$ L PCR product and primer sets modified with an 8 bp  
35 249 multiplexing identifier (MID) adaptor used for barcode tagging, thereby allowing for post-sequencing  
36 250 separation of the samples, using the above PCR conditions. Each sediment sample was amplified in

1  
2  
3 251 triplicate, the triplicates pooled, cleaned using the Agencourt AMPure XP Purification System  
4 252 (Beckman Coulter, Bromley, UK) and the concentration of each product calculated using the  
5 253 PicoGreen assay (Invitrogen) against standard DNA curves with  $r^2 \geq 0.99$ . DNA libraries were  
6 254 prepared for sequencing using the Roche emPCR Method Manual – Lib-L MV and the Roche  
7 255 Sequencing Method Manual for the GS FLX Titanium Series. Picotitre plates were used with an 8 lane  
8 256 gasket. Data was processed using QIIME (Caporaso et al. 2010). Sequences were first de-multiplexed,  
9 257 denoised and chimeras removed using Ampliconnoise (Quince et al. 2011), and clustered at 97 %  
10 258 sequence similarity using Uclust. Representative sequences were PYNAST aligned and taxonomy  
11 259 assigned using the Silva database version 108 (Pruesse et al. 2007). This assigned 87.7 % of bacterial  
12 260 sequences and 87.2 % archaeal sequences to Order level. Sequence data is available at the EMBL  
13 261 database (accession number ERP002371).  
14 262

15 263 A total of 109582 high quality sequences were obtained for the 12 sediment cores examined,  
16 264 ranging from 5237 to 15424 per sample with an average read length across all samples of 375 bp  
17 265 (Supplementary Table 1). The ratio of archaeal:bacterial sequences obtained from each core was  
18 266 similar to the values obtained from the qPCR (Supplementary Table 1), and so the archaeal and  
19 267 bacterial data-sets were combined, OTUs picked at 97% sequence similarity and the data set  
20 268 randomly sub-sampled so each sample contained the same number of sequences (5237).  
21 269

## 22 270 *Statistics*

23 271 For qPCR data (Figure 3), all error bars are standard deviation (n = 5). Two-way ANOVA was used to  
24 272 test for differences in the quantity of 16S rRNA copy numbers followed by post-hoc tests to identify  
25 273 pH treatments with significantly different abundances. For the 16S rRNA tagged 454 pyrosequencing  
26 274 data set the Qiime pipeline and Primer vs 6.1 multivariate analysis software (Clarke and Gorley,  
27 275 2006) were used to calculate alpha diversity for each clone library. Resemblances between samples  
28 276 were generated using the Bray-Curtis coefficient, calculated using both the abundance and the  
29 277 presence and absence of OTUs. Non-metric multidimensional scaling (MDS) was applied to assess  
30 278 the grouping structure of samples and their corresponding pH treatment. An analysis of similarity  
31 279 (ANOSIM) was used to determine the effect of pH on community composition.  
32 280

33 281

## 34 282 **Results**

35 283 *Measurements of environmental parameters*  
36  
37  
38  
39  
40  
41  
42  
43  
44  
45  
46  
47  
48  
49  
50  
51  
52  
53  
54  
55  
56  
57  
58  
59  
60

1  
2  
3 284 pH remained relatively stable throughout the 10 weeks, with a maximum standard deviation of 0.3  
4 285 pH (across cores) found at the lower pH conditions (Table 1). Temperature and salinity remained  
5 286 constant varying by an average of 0.6 °C and 0.47, respectively (Table 1). Total alkalinity was more  
6 287 variable between the cores, resulting in relatively high standard deviations for each treatment,  
7 288 **however, there was no significant differences** between treatments. The low pH and high alkalinity  
8 289 values resulted in high carbon conditions (see pCO<sub>2</sub> and DIC values in Table 1), and the saturation  
9 290 state for aragonite was near or below 1 in all cores below pH 7.5 (Table 1). Also shown are nutrient  
10 291 concentrations: there were no differences between treatments for each nutrient measured.  
11  
12  
13  
14  
15  
16

292

### 293 *pH impact on the flux of silicate from the sediment to the water column*

17  
18  
19 294 Although there was a shift in the flux of **dissolved inorganic nitrogen (DIN)** through the course of the  
20 295 experiment, going from a source at week 2 to a sink at week 10 (results not shown), with the  
21 296 exception of silicate (Figure 1), there was no significant relationship between pH and the flux of  
22 297 nutrients (ammonia, nitrate, nitrite or phosphate) measured over a 24 h period after 2 and 10 weeks  
23 298 incubation (results not shown). There was a positive flux for silicate at week 2 and week 10. pH had  
24 299 no impact on silicate flux at week 2 (one-way ANOVA  $F = 0.12$ ;  $p = 0.972$ ) (results not shown), but  
25 300 there was a significant decrease in the flux of silicate from the sediment to the water column in the  
26 301 pH 7.0 and 7.5 treatments **when compared to the other treatments** (one-way ANOVA  $F = 3.24$ ;  $p =$   
27 302  $0.033$ ) (Figure 1).  
28  
29  
30  
31  
32  
33

303

### 304 *Identification of the composition of the microphytobenthos mat*

34  
35 305 The pink-pigmented mat appeared in cores receiving seawater adjusted to pH 7.0 and 7.5 after five  
36 306 weeks incubation, peaked at eight weeks (Figure 2A), but was still visible in small patches after ten  
37 307 weeks in the cores exposed to pH 7.0 seawater. No pink colouration was evident on sediment cores  
38 308 receiving ambient pH seawater (Figure 2B), or cores receiving seawater adjusted to pH 6.0 and 6.5.  
39 309 Examination under a microscope revealed the presence of a community mainly comprising pink  
40 310 filamentous **Cyanobacteria** and diatoms (Figure 2C). From the microscope analysis, the same  
41 311 community appeared to be present within all samples analysed from both pH 7.0 and pH 7.5 cores.  
42 312 Analysis of sequence data obtained from clone libraries of PCR-amplified **Cyanobacteria** and  
43 313 chloroplast 16S rRNA gene sequences revealed the **Cyanobacteria** to be *Spirulina* sp., and diatoms of  
44 314 the Orders **Naviculales** (OTUs 1) and **Bacillariales** (OTUs 2 and 3) (Figure 2D). No other  
45 315 cyanobacterium other than *Spirulina* was detected in the clone library. OTU 1, most closely related  
46 316 to a *Navicula* sp., was the most abundant diatom detected (50% of sequences). Although OTUs 1, 2  
47 317 and 3 could be detected in samples taken on day 0, no *Spirulina* sp. sequences were detected,  
48  
49  
50  
51  
52  
53  
54  
55  
56  
57  
58  
59  
60

1  
2  
3 318 suggesting that this particular species may have colonised the shell gravel from the seawater  
4 319 overlying the sediment cores in the mesocosm.

5  
6 320

7  
8 321 *pH impacts on the abundance of 16S rRNA*

9 322 The activity of *Cyanobacteria* and micro-algae within the different treatments was compared using  
10 323 qPCR. Measurements with PCR primers specific for *Cyanobacteria* and chloroplast 16S rRNA revealed  
11 324 both significant changes with pH treatment and when the week 2 and week 10 measurements were  
12 325 compared, but differences in the pH response at week 2 and weeks 10 were also evident (Figure 3A).  
13 326 At week 2, *Cyanobacteria* 16S rRNA abundance increased in the pH 6.5, 7.0 and 7.5 treatments, but  
14 327 the abundance in the pH 6.0 was not significantly different to the value in the control sediments. At  
15 328 week 10, increases in 16S rRNA abundance were evident only in the pH 7.0 and 7.5 treatments and  
16 329 was equivalent to an 295% and 690% increase in abundance of cyanobacterial 16S rRNA,  
17 330 respectively, when compared to the pH 8.0 treatments. This is indicative of a substantial increase in  
18 331 the activity of *Cyanobacteria* and micro-algae within the pH 7.0 and pH 7.5 treatments. Similar  
19 332 profiles were evident for measurements of bacterial 16S rRNA (Figure 3B).

20  
21 333

22 334 *Detailed comparison of the microbial community structure within the pH 7.0, pH 7.5 and pH 8.0*  
23 335 *treatments*

24 336 Although the number of OTUs and measures of species richness (Figure 4A) did not differ between  
25 337 pH treatments, there was a significant drop for measurements of Shannon diversity (Figure 4B) and  
26 338 Pielou evenness (Figure 4C) within the pH 7.0 treatments (one-way ANOVA  $F = 7.39$ ;  $p = 0.013$  and  $F =$   
27 339  $8.24$ ;  $p = 0.009$ , respectively). This suggests that although the same OTUs were present in all  
28 340 treatments, the low pH cores may have become numerically dominated by a small subset of OTUs.  
29 341 To compare community composition within the different sediment cores, resemblance matrices  
30 342 were generated using the Bray-Curtis coefficient, calculated using both the abundance and also the  
31 343 presence/absence of OTUs. Bray-Curtis abundance matrices indicated significant differences  
32 344 between pH treatments (ANOSIM  $R = 0.274$ ;  $p = 0.035$ ), whereas the resemblance matrices  
33 345 generated using the presence/absence data sets indicated no differences between treatments  
34 346 (ANOSIM  $R = 0.009$ ;  $p = 0.143$ ), confirming that the changes in community structure were driven by  
35 347 changes in the relative abundances of OTUs rather than by the presence or absence of different  
36 348 OTUs in each of the pH treatments. Multidimensional scaling ordination analysis revealed  
37 349 considerable overlap between the structure of the microbial communities from the pH 8.0 and pH  
38 350 7.5 treatments, but that the pH 7.0-treated cores differed (Figure 5A). Post-hoc tests confirmed the  
39 351 pH 7.0 treatments were significantly different to the pH 8.0 and pH 7.5 cores (comparisons of pH 7.0

1  
2  
3 352 and 7.5  $R = 0.354$ ,  $p = 0.029$ ; pH 7.0 and pH 8.0  $R = 0.521$ ,  $p = 0.029$ ; pH 7.5 and pH 8.0  $R = -0.094$ ,  $p =$   
4 353 0.657). Together, this suggests that there were key changes to the relative abundance of dominant  
5  
6 354 OTUs within the pH 7.0-treated cores, and that there may have been phylogenetic structure to these  
7  
8 355 changes.

9 356  
10  
11 357 When the OTUs were grouped at Class-level taxonomy, nine Classes were seen to have abundances  
12 358 greater than 2 % within the data-set (in order of most abundant: Chloroplasts, Subsection III of the  
13 359 *Cyanobacteria*, *Alphaproteobacteria*, *Gammaproteobacteria*, *Deltaproteobacteria*, Marine Group I  
14 360 (*Thaumarchaeota*), the *Planctomycete* Classes OM190 and *Planctomycetia* and the  
15 361 *Gemmatimonadetes*). Of these nine, five showed significant increases or decreases within the pH 7.0  
16 362 cores (Figure 5B). The relative abundance of chloroplast and *Cyanobacteria* Sub-section III sequences  
17 363 more than doubled at pH 7.0 when compared to the pH 8.0 and pH 7.5 treatments. In contrast, the  
18 364 *Alphaproteobacteria*, *Planctomycetes* Class OM190 and the *Thaumarchaeota* Marine Group I all  
19 365 decreased with decreasing pH (Figure 5B). When these differences were examined in more detail,  
20 366 the changes to the relative abundance of the Classes Chloroplast, Subsection III and Marine Group I  
21 367 were mainly due to changes in the relative abundance of single OTUs (Figure 5C). For Subsection III,  
22 368 the relative abundance of an OTU most closely related to *Spirulina* sp. and within the Chloroplasts,  
23 369 an unidentified diatom (OTU #5248), closely related to OTU 1 (*Navicula* sp.) identified in Figure 2D,  
24 370 both increased in abundance within the pH 7.0 treatments. An uncultured *Nitrosopumilus* (OTU  
25 371 #7731) was mostly responsible for the decreases in relative abundance seen for the Marine Group I  
26 372 Class. These OTUs were first, second and fourth most abundant OTUs within the entire data-set. The  
27 373 third most abundant, OTU #4558, very similar to the diatom most closely related to *Psammodictyon*  
28 374 *panduriforme* (OTU 3) identified in Figure 2D, did not differ with pH (results not shown). The fifth  
29 375 most abundant OTU belonged to the *Rhodospirillales*. Although the relative abundance of this  
30 376 particular OTU did not differ between pH treatments (Figure 5C), the changes to the  
31 377 Alphaproteobacteria could be traced to a decrease in the relative abundance of members of the  
32 378 family *Rhodospirillaceae*. There were significant decreases in the relative abundance of this family  
33 379 in both the pH 7.0 and 7.5 treatments when compared to the pH 8.0 cores (one-way ANOVA  $F =$   
34 380 9.43;  $p = 0.006$ ).

35  
36  
37 381

## 38 382 Discussion

39 383 This mesocosm study clearly demonstrated that a CO<sub>2</sub>-induced decrease in the pH of seawater to  
40 384 either 7.5 or 7.0 resulted in a transient bloom of benthic *Cyanobacteria* and diatoms, predominantly  
41 385 consisting of the cyanobacterium *Spirulina* sp. and diatom species (Figures 2 and 5). Although the  
42  
43  
44  
45  
46  
47  
48  
49  
50  
51  
52  
53  
54  
55  
56  
57  
58  
59  
60

1  
2  
3 386 bloom appeared visually to have begun to die back by week 10 of the experiment, qPCR  
4 387 measurements of 16S rRNA specific for *Cyanobacteria* (Figure 3) and detailed analysis of the  
5 388 community composition indicated increased abundance of the *Spirulina* sp. and a diatom most  
6 389 closely related to *Navicula* sp. within the pH 7.0 treatments (Figures 5c). Also evident were changes  
7 390 to the composition of the active bacterial and archaeal community, including decreases to the  
8 391 relative abundance of *Rhodospirillales*, *Planctomycetes* Class OM190 and *Thaumarchaeota* (Figure  
9 392 5). A decrease in the flux of silicate from the sediment to the water column under these pH  
10 393 conditions was also evident (Figure 1), perhaps indicating increased uptake of silicate by diatoms to  
11 394 support growth and reproduction, or due to the increased adsorption of silicate onto hydrated metal  
12 395 oxides. This is known to occur within sediments under the oxic conditions brought about by the  
13 396 activity of microphytobenthos (Hartikainen et al. 1996).

14 397  
15 398 Although the diatom species could be detected within pre-exposure sediments, it is possible that the  
16 399 *Spirulina* sp. was introduced from the overlying seawater used to feed the sediment cores within  
17 400 different concentrations of CO<sub>2</sub>. The composition of microphytobenthos has been shown to vary  
18 401 with sediment type. Although they are predominantly composed of diatoms, previous studies have  
19 402 recorded high incidences of *Cyanobacteria* on coarse grain sediments (Waterman et al. 1999), and  
20 403 Franks and Stolz (2009) showed that newly colonised sands were mainly comprised of *Oscillatoria*  
21 404 sp. and *Spirulina* sp., indicating that this species readily colonised coarse grain sediments such as  
22 405 those used within this experiment. Experiments designed to trial the efficiency of *Spirulina* sp. for  
23 406 CO<sub>2</sub> sequestration have also shown this cyanobacterium to increase biomass and CO<sub>2</sub> fixation rates  
24 407 within photobioreactors receiving 6 % CO<sub>2</sub> (de Rosa et al. 2011), suggesting that members of this  
25 408 Genus are well-equipped to thrive under elevated CO<sub>2</sub> conditions.

26 409  
27 410 Studies of the impact of elevated CO<sub>2</sub> on *Cyanobacteria* within biofilm communities have shown  
28 411 members of the Chroococcales to increase in abundance (Russell et al. 2013; Taylor et al. 2014), and  
29 412 enhance inorganic uptake and growth for a number of phytoplankton groups, including the  
30 413 *Cyanobacteria* *Trichodesmium* (Hutchins et al. 2007; Levitan et al. 2007; Lomas et al. 2012) and  
31 414 diatoms (e.g. Tortell et al. 2008; Trimborn et al. 2009; Sun et al. 2011). Both the *Spirulina* sp. and  
32 415 *Navicula* sp. increased in abundance within the pH 7.0 and 7.5 treatments, and these were  
33 416 presumably responding to an increase in pCO<sub>2</sub> concentration. However, the relative abundance of  
34 417 the OTU most closely related to *Psammodictyon panduriforme* did not differ between the pH  
35 418 treatments (Figure 5). This difference may be, in part, related to the carbon concentrating  
36 419 mechanisms (CCMs) used by marine *Cyanobacteria* and micro-algae. Due to the inefficiencies of the

1  
2  
3 420 key carbon fixing enzyme, RubisCO (ribulose-1,5-bisphosphate carboxylase/oxygenase), many  
4 421 phytoplankton species, including diatoms and *Cyanobacteria* have evolved CCMs to elevate  
5 422 intracellular concentrations of CO<sub>2</sub>, but at an energy cost (reviewed by Reinfelder, 2011). It has been  
6 423 suggested that phytoplankton that rely on diffusive entry of CO<sub>2</sub> or those that are able to suppress  
7 424 their CCMs may have a selective advantage under elevated CO<sub>2</sub> conditions (Raven, 1991). Laboratory  
8 425 studies have indicated that many diatoms possess relatively efficient CCMs that are strongly  
9 426 regulated by CO<sub>2</sub> concentration (Burkhardt et al. 2001; Rost et al. 2003; Trimborn et al. 2009;  
10 427 Hopkinson et al. 2011). However, diatoms utilise a high diversity of methods to acquire carbon  
11 428 (Reinfelder et al. 2011), and so species specific responses to elevated levels of CO<sub>2</sub> may be detected  
12 429 (Kim et al. 2006; Trimborn et al. 2009; Torstensson et al. 2012). Our results are similar to the  
13 430 response of the pelagic mesocosm of Kim et al. (2006) where an increase in the specific growth rate  
14 431 of *Skeletonema costatum* was observed at 750 µatm CO<sub>2</sub>, but there was no effect on the growth rate  
15 432 of *Nitzschia* spp.

16 433  
17 434 Alternatively, the lack of response of the *Psammodictyon* sp. may have been due to pH changes  
18 435 brought about by the decrease in pH rather than an increase in CO<sub>2</sub> concentration. Several diatom  
19 436 taxa have a statistically significant relationship with pH, and this has been exploited in the use of  
20 437 diatom community composition as an ecological indicator for monitoring environmental change in  
21 438 lakes, and to reconstruct past lake-water pH (Birks et al. 1990). In a review of literature published on  
22 439 the effects of pH on marine phytoplankton growth under laboratory conditions, some species were  
23 440 able to grow at a wide range of pH, whereas others had growth rates that varied greatly over a 0.5 to  
24 441 1.0 pH unit change: pH can inhibit growth regardless of CO<sub>2</sub> concentration for some phytoplankton  
25 442 species (Hinga 2002).

26 443  
27 444 The presence of microphytobenthos has been shown to increase the lability of sediment organic  
28 445 matter and as a result, increase bacterial abundance (Hardison et al. 2013). This would be expected  
29 446 to alter the activity of archaea and bacteria within the sediment surface. Within this study, we have  
30 447 shown that in conjunction to the increase to the *Spirulina* sp. and *Navicula* sp., there was a  
31 448 corresponding decrease in the relative abundance of 16S rRNA sequences most closely related to the  
32 449 Alphaproteobacteria (which could be traced to a decrease in the Family *Rhodospirillaceae*), the  
33 450 Planctomycete Class OM190 and the *Thaumarchaeota* Marine Group I (Figure 5c). The decrease to  
34 451 the *Thaumarchaeota* was mainly due to the decrease in the relative abundance of a single  
35 452 *Nitrosopumilus* sp. (Figure 5). These archaea are known aerobic ammonia oxidisers, converting  
36 453 ammonia to nitrite. However, it is known that pH treatment had no impact on ammonia oxidising

1  
2  
3 454 within this mesocosm experiment: Kitidis et al. (2011) reported no differences to ammonia oxidising  
4 455 rates between pH treatments. However, ammonia oxidising bacteria may also have been present:  
5  
6 456 the relative contribution of bacteria and archaea to nitrification within these sediments is not  
7  
8 457 known. While some archaeal ammonia oxidisers can tolerate a wide range of oxygen levels, others  
9  
10 458 appear to be more suited to low-oxygen environments (Erguder et al. 2009). It may be possible that  
11  
12 459 the archaeal ammonium oxidisers present within the sediments within this study preferred lowered  
13  
14 460 oxygen concentrations and were sensitive to the presumably high levels of oxygen produced by the  
15  
16 461 photosynthetic activities of the dominant *Cyanobacteria* and diatom species. The *Rhodospirillaceae*  
17  
18 462 contain the purple non-sulphur bacteria, common inhabitants of microphytobenthos mats. This  
19  
20 463 group of bacteria are anaerobic anoxygenic phototrophs, typically using hydrogen as a reducing  
21  
22 464 agent during photosynthesis (Hubas et al. 2011). The purple non-sulphur bacteria migrate away from  
23  
24 465 oxygen (Hubas et al. 2011), and it is also possible that the high levels of oxygen presumably  
25  
26 466 produced by the photosynthetic activity of *Cyanobacteria* and diatoms within the biofilm resulted in  
27  
28 467 a decrease in this group. Members of the OM190 have been detected in a variety of marine  
29  
30 468 environments, and are commonly found associated with algae (Rappe et al., 1997; Bengtson &  
31  
32 469 *Ovreas, 2010*). But as no cultured representative of this deeply branching group currently exists,  
33  
34 470 there is very little knowledge on the function of this group within marine ecosystems. Interestingly,  
35  
36 471 the relative abundance of the class *Planctomycetacia* was shown to increase with increasing pCO<sub>2</sub>  
37  
38 472 concentration in a previous benthic mesocosm studying the impact of elevated pCO<sub>2</sub> on Arctic  
39  
40 473 sediment microbial communities (Tait et al. 2013). More information is required on the function of  
41  
42 474 the members of the *Planctomyces* within marine sediments to understand the impact of elevated  
43  
44 475 CO<sub>2</sub> on this group, and the possible consequences for the biogeochemical cycling on nutrients within  
45  
46 476 marine sediments.

47  
48 477  
49  
50 478 The microphytobenthos bloom was most evident in the pH 7.0 and 7.5 cores after 6 weeks, peaked  
51  
52 479 at 8 weeks but had declined by week 10, being only visible in small patches in the pH 7.0 cores. The  
53  
54 480 dense layer of diatoms and *Cyanobacteria* at the sediment surface may have depleted essential  
55  
56 481 nutrients, causing a crash in the microphytobenthos population. Alternatively, an increase in grazing  
57  
58 482 by meiofauna may have resulted in the decrease in microphytobenthos. Microphytobenthos are an  
59  
60 483 important food source for meiofauna in intertidal environments (Miller et al., 1996). Although  
484  
485 484 acidification did not change meiofauna abundance in the pH 7.0 or 7.5 treatments when compared  
486  
487 485 to the pH 8.0 controls (Jeroen Ingels, personal communication), a number of studies have now  
488  
489 486 shown that many invertebrates cope with elevated CO<sub>2</sub> by use of energetically expensive

1  
2  
3 487 physiological processes (Findlay et al. 2010; Stumpp et al. 2012) and as a result may consume more  
4 488 food per individual (Thomsen et al. 2013).

5 489  
6  
7  
8 490 There was a significant increase in the abundance of cyanobacterial 16S rRNA within the pH 6.5  
9 491 cores at week 2, but at week 10 the abundance of cyanobacterial 16S rRNA within both the pH 6.0  
10 492 and 6.5 treatments did not differ to the pH 8.0 cores (Figure 3). Although there was a shift in the flux  
11 493 of DIN through the course of the experiment, going from a source at week 2 to a sink at week 10,  
12 494 there were no significant differences between pH treatments for both DIN and dissolved inorganic  
13 495 phosphate fluxes. The levels of nutrients measured within the seawater above the cores also  
14 496 indicated that there were no differences to the nutrient concentrations with pH (Table 1), and so it is  
15 497 unlikely that the pH 6.0 and 6.5 cores were nutrient limited. Again, this may have been due to  
16 498 increased grazing by meiobenthos under the high CO<sub>2</sub> conditions. Alternatively, it is conceivable that  
17 499 the CO<sub>2</sub>-induced low pH directly impacted the growth of microphytobenthos bloom within the pH  
18 500 6.0 and 6.5 treatments. Although both *Spirulina* sp. and diatoms are capable of growing at a range of  
19 501 pH, including < pH 6.0 for certain species in laboratory cultures (Ramanan et al. 2010; Hinga, 2002)  
20 502 within our mesocosm, it is possible that a decrease in pH to values as low as pH 6.0 and 6.5 may  
21 503 have indirectly impacted the microbial activity. For example, during the CO<sub>2</sub> release experiment in  
22 504 Ardmucknish Bay, there was increased dissolution of minerals, including several toxic species  
23 505 (Lichtschlag et al. manuscript under review) and this was thought to have caused a decrease in the  
24 506 abundance of microbial 16S rRNA genes (Tait et al. 2015). For the diatom species, silicon  
25 507 biomineralisation may also be problematic within low pH environments (Hervé et al. 2012).

26 508  
27 509 There is a need to understand the impacts of a CO<sub>2</sub> leak on the surrounding environment. In  
28 510 addition, the European Commission (EC) directive (2009/31/EC) on geological storage of CO<sub>2</sub>  
29 511 requires the establishment of a framework for the detection of CO<sub>2</sub> seep. An increased  
30 512 understanding of the possible scenarios triggered by CO<sub>2</sub> leaks could lead to low-cost strategies for  
31 513 monitoring CO<sub>2</sub>. The QICS project concluded that the use of autonomous underwater vehicles  
32 514 equipped with a range of sensors, including both chemical and acoustic (for gas bubbles) would be a  
33 515 useful monitoring strategy (Blackford et al, 2014). Monitoring for blooms of microphytobenthos may  
34 516 also prove to be a low-cost, additional indicator of a CO<sub>2</sub> leak from injection pipeline failure in  
35 517 coastal areas. Along with direct observation, this could be monitored via chlorophyll pigment  
36 518 analysis of surface sediments. However, it is essential that these approaches are applied in  
37 519 conjunction with detailed, seasonal, baseline studies of potential CO<sub>2</sub> storage sites to determine  
38 520 natural variability in both the biology, but also natural variability in CO<sub>2</sub> levels. In addition, continued

1  
2  
3 521 comparisons to a nearby reference site of similar sediment characteristic and water depth would  
4 522 also be essential to untangle natural, temporal (both seasonal and diurnal) changes to the  
5  
6 523 microphytobenthos community from those caused by CO<sub>2</sub> leakage.  
7  
8 524

9 525 **Conclusions**

10  
11 526 The current study has demonstrated a clear impact to the microbial community, specifically an  
12  
13 527 increase to primary producers, creating a visible bloom of *Spirulina* and diatom species. However  
14  
15 528 although two diatom species dominated the surface sediment microbial communities, only one  
16  
17 529 species, most closely related to a *Navicula* sp. also increased in abundance within the pH 7.0  
18  
19 530 treatments. More studies are required to understand the underlying mechanisms in the response of  
20  
21 531 benthic *Cyanobacteria* and micro-algae to elevated levels of CO<sub>2</sub>, including the possible role of  
22  
23 532 carbon concentrating mechanisms and differences in sensitivities to pH. The microphytobenthos  
24  
25 533 bloom did not occur within the pH 6.0 or 6.5 treatments and again more study is required to  
26  
27 534 understand why this ~~is~~ occurred. Possibilities include increased grazing by meiobenthos, the release  
28  
29 535 of toxic metals, as indicated by the Ardmucknish Bay field experiment (Lichtsschlag et al. manuscript  
30  
31 536 under review), impacts to silicon biomineralisation or combinations of all of these factors. The  
32  
33 537 abundance of photosynthetic microbes could prove to be an effective biological indicator for the  
34  
35 538 detection and monitoring of CO<sub>2</sub> leaks within specific locations, such as pipelines within coastal  
36  
37 539 areas.  
38  
39  
40  
41  
42  
43  
44  
45  
46  
47  
48  
49  
50  
51  
52  
53  
54  
55  
56  
57  
58  
59  
60

540 **Acknowledgements**

541 The molecular characterisation of the microbial communities was supported through PML internal  
542 Research Project funding (PML RP) and we are grateful to Roche for the generous loan of a 454 GS  
543 Flx sequencer and materials required for both the preparation and sequencing of samples used in  
544 this study. The setting up and running of the mesocosm was funded by the European Project RISCs  
545 (European Community's Seventh Framework Programme (FP7/2007-2013) under grant agreement  
546 no. EU FP7 240837. HSF was in receipt of Lord Kingsland PML Fellowship. Thanks to the crew of  
547 Quest for collecting the sediment, Malcolm Woodward for overseeing the nutrient analysis and to  
548 Paul Somerfield for guidance on statistical analysis.

For Peer Review

549 **References**

- 550 Atamanchuk D, Tengberg A, Aleynik D, Fietzek P, Hall POJ, Shitashima K & Stahl H (2015) Field-testing  
551 of methods and strategies to detect CO<sub>2</sub> leakage from a simulated sub-seabed storage site.  
552 *Int J Greenh Gas Control* In Press.
- 553 Beaufort L, Probert I, de-Garidel-Thoron T, Bendriff EM, Ruiz-Pino D, Metzl N, Goyet C, Buchet N,  
554 Coupel P, Grelaud M, Rost B, Rickaby REM & de Vargas C (2011) Sensitivity of  
555 coccolithophores to carbonate chemistry and ocean acidification. *Nature* 476: 80-83.
- 556 Beman JM, Chow CE, King AL, Feng Y, Fuhrman JA, Andersson A, Bates NR, Popp BN & Hutchins D  
557 (2011) Global declines in oceanic nitrification rates as a consequence of ocean acidification.  
558 *Proc Nat Acad Sci USA* 108: 208-213.
- 559 Birks HJB, Line JM, Juggins S, Stevenson AC & Ter Braak CJF (1990) Diatoms and pH reconstruction.  
560 *Philos T R Soc A*, 327: 263-278.
- 561 Blackford JC, Jones N, Proctor R & Holt J (2008) Regional scale impacts of distinct CO<sub>2</sub> additions in the  
562 North Sea. *Mar Pollut Bull* 56: 1461–1468.
- 563 Blackford JC, Jones N, Proctor R, Holt J, Widdicombe S, Lowe D & Rees A (2009) An initial assessment  
564 of the potential environmental impact of CO<sub>2</sub> escape from marine carbon capture and  
565 storage systems. *Proc Inst Mech Eng A: J Power Energy* 223: 269–280.
- 566 Blackford JC, Stahl H, Bull JM, Bergès BJP, Cevatoglu M, Lichtschlag, A. et al. (2014) Detection and  
567 impacts of leakage from sub-seafloor Carbon Dioxide Storage. *Nature Climate Change* 4:  
568 1011–1016.
- 569 Brewer PG & Riley JP (1965) The automatic determination of nitrate in seawater. *Deep Sea Res* 12:  
570 765–772.
- 571 Burkhardt S, Amoroso F, Riebesell U & Sültemeyer DU (2001) CO<sub>2</sub> and HCO<sub>3</sub><sup>-</sup> uptake in marine  
572 diatoms acclimated to different CO<sub>2</sub> concentrations. *Limnol Oceanogr* 46: 1378–1391.
- 573 Caporaso JG, Kuczynski J, Stombaugh J, Bittinger K, Bushman FD, Costello EK et al (2010) QIIME  
574 allows analysis of high-throughput community sequencing data. *Nature Methods* 7: 335-336.
- 575 Clarke KR & Gorley RN (2006) PRIMER v6: User Manual/Tutorial. PRIMER-E: Plymouth, UK.
- 576 Coolen MJL, Abbas B, van Bleijswijk J, Hopmans EC, Kuypers MMM, Wakeman SG & Sinninge Damsté  
577 JS (2007) Putative ammonia-oxidizing Crenarchaeota in suboxic waters of the Black Sea: a  
578 basin-wide ecological study using 16S ribosomal and functional genes and membrane lipids.  
579 *Environ Microbiol* 9: 1001-1016.
- 580 da Rosa APC, Carvalho LF, Goldbeck L, Costa JAV (2011) Carbon dioxide fixation by microalgae  
581 cultivated in open bioreactors. *Energy Conversion and Management* 52: 3071-3073.

- 1  
2  
3 582 Dickson AG & Millero FJ (1987) A comparison of the equilibrium constants for the dissociation of  
4 583 carbonic-acid in seawater media. *Deep-Sea Res* 34: 1733-1743.
- 5  
6 584 Dickson AG (1990) Thermodynamics of the dissociation of boric acid in potassium-chloride solutions  
7 585 form 273.15 K to 318.15 K. *J Chem Thermodyn* 22: 113-127.
- 8  
9 586 Dickson AG, Sabine CL & Christian JR (2007) Guide to best practices for ocean CO<sub>2</sub> measurements.  
10 587 PICES special publication, 3.
- 11  
12 588 Erguder TH, Boon N, Wittebolle L, Marzorati M & Verstraete W (2009) Environmental factors shaping  
13 589 the ecological niches of ammonia-oxidizing archaea. *FEMS Microbiol Rev* 33: 855-869.
- 14  
15 590 Findlay HS, Kendall MA, Spicer JI & Widdicombe S (2010) Relative influences of ocean acidification  
16 591 and temperature on intertidal barnacle post-larvae at the northern edge of their geographic  
17 592 distribution. *Estuar Coast Shelf Sci* 86: 675-682.
- 18  
19 593 Franks J & Stolz JF (2009) Flat laminated microbial mat communities. *Earth Sci Rev* 96: 163-172.
- 20  
21 594 Fu FX, Mulholland MR, Garcia NS, Beck A, Bernhardt PW, Warner ME, Sañudo-Wihelmy SA &  
22 595 Hutchins DA (2008) Interactions between changing pCO<sub>2</sub>, N<sub>2</sub> fixation, and Fe limitation in the  
23 596 marine unicellular cyanobacterium *Crocospaera*. *Limnol Oceanogr* 53: 2472-2484.
- 24  
25 597 Global CCS Institute (2012) Global status of CCS.  
26 598 <http://www.globalccsinstitute.com/publications/global-status-ccs-2012>
- 27  
28 599 Grasshoff K (1976) Methods of Seawater Analysis. Verlag Chemie, Weinheim.
- 29  
30 600 Hartikainen H, Pitkänen M, Kairesalo T & Tuominen L (1996) Co-occurrence and potential chemical  
31 601 competition of phosphorus and silicon in lake sediment. *Water Research* 30: 2472-2478.
- 32  
33 602 Håvelsrud OE, Haverkamp TH, Kristensen T, Jakobsen KS & Rike AG (2012) Metagenomic and  
34 603 geochemical characterization of pockmarked sediments overlaying the Troll petroleum  
35 604 reservoir in the North Sea. *BMC Microbiol* 12, 203.
- 36  
37 605 Håvelsrud OE, Haverkamp TH, Kristensen T, Jakobsen KS & Rike AG (2013) Metagenomics in CO<sub>2</sub>  
38 606 monitoring. *Energy Procedia* 37, 4215-4233.
- 39  
40 607 Hervé V, Derr J, Douady S, Quinet M, Moisan L & Lopez PJ (2012) Multiparametric Analyses Reveal  
41 608 the pH-Dependence of Silicon Biomineralization in Diatoms. *PLoS One* 7: e46722.
- 42  
43 609 Hinga KR (2002) Effects of pH on coastal marine phytoplankton. *Mar Ecol Prog Ser* 238: 280-300.
- 44  
45 610 Holloway S (2007) Carbon dioxide capture and geological storage. *Philos T R Soc A* 365: 1095-1107.
- 46  
47 611 Hopkinson BM, Dupont CL, Allen AE & Morel FM (2011) Efficiency of the CO<sub>2</sub>-concentrating  
48 612 mechanism of diatoms. *P Natl Acad Sci* 108: 3830-3837.
- 49  
50 613 Hubas C, Jesus B, Passarelli C & Jeanthon C (2011) Tools providing new insight into coastal  
51 614 anoxygenic purple bacterial mats: review and perspectives. *Res microbiol* 162: 858-868.
- 52  
53  
54  
55  
56  
57  
58  
59  
60

- 1  
2  
3 615 Huse SM, Welch DM, Morrison HG & Sogin ML (2010) Ironing out the wrinkles in the rare biosphere  
4 616 through improved OTU clustering. *Environ Microbiol* 12: 1889-1898.  
5  
6 617 Hutchins DA, Fu F, Zhang Y, Warner ME & Feng Y (2007) CO<sub>2</sub> control of *Trichodesmium* N<sub>2</sub> fixation,  
7 618 photosynthesis, growth rates, and elemental ratios: Implications for past, present, & future  
8 619 ocean biogeochemistry. *Limnol Oceanogr* 52: 1293-1304.  
9  
10 620 Ishida H, Watanabe Y, Fukuhara T, Kaneko S, Furusawa K & Shirayama Y (2005) In situ enclosure  
11 621 experiment using benthic chamber system to assess the effect of high concentration of CO<sub>2</sub>  
12 622 on deep-sea benthic communities. *J Oceanogr* 61: 835–843.  
13  
14 623 Ishida H, Gomen LG, West J, Krüger M, Coombs P, Berge JA, Fukuhara T, Magi M & Kita J (2013)  
15 624 Effects of CO<sub>2</sub> on benthic biota: An *in situ* benthic chamber experiment in Storfjorden  
16 625 (Norway). *Mar Pollut Bull* 73: 443-51.  
17  
18 626 Kerfahi D, Hall-Spencer JM, Tripathi BM, Milazzo M, Lee J & Adams JM (2014) Shallow water marine  
19 627 sediment bacterial community shifts along a natural CO<sub>2</sub> gradient in the Mediterranean Sea  
20 628 off Vulcano, Italy. *Microb Eco* 67: 819-828.  
21  
22 629 Kim JM, Lee K, Shin K, Shin K, Kang JH, Lee HW, Kim M, Jang PG, Jang MC (2006) The effect of  
23 630 seawater CO<sub>2</sub> concentration on growth of a natural phytoplankton assemblage in a  
24 631 controlled mesocosm experiment. *Limnol Oceanogr* 51: 1629–1636.  
25  
26 632 Kirkwood D (1989) Simultaneous determination of selected nutrients in seawater. International  
27 633 Council for the Exploration of the Sea (ICES), CM 1989/C:29.  
28  
29 634 Kitidis V, Laverock B, McNeil CL, Beesley A, Cummings D, Tait K, Osborn AM, Widdicombe S (2011)  
30 635 The impact of ocean acidification on sediment nitrification. *Geophysical Research Letters*.  
31 636 doi:10.1029/2011GL049095.  
32  
33 637 Komárek J, Hauer T (2010) CyanoDB. cz—on-line database of cyanobacterial genera. World-Wide  
34 638 Electronic Publication, University of South Bohemia & Institute of Botany AS CR.  
35  
36 639 Langer G, Nehrke G, Probert I, Ly J, Ziveri P (2009) Strain-specific responses of *Emiliana huxleyi* to  
37 640 changing seawater carbonate chemistry. *Biogeosci Discuss* 6: 4361–4383.  
38  
39 641 Levitan O, Brown C, Sudhaus S, Campbell DA, LaRoche J, Berman-Frank I (2010) Regulation of  
40 642 nitrogen metabolism in the marine diazotroph *Trichodesmium* IMS101 under varying  
41 643 temperatures and atmospheric CO<sub>2</sub> concentrations. *Environ Microbiol* 12: 1899–1912.  
42  
43 644 Lichtschlag A, James RH, Stahl H & Connelly D (2015) Effect of a controlled sub-seabed release of  
44 645 CO<sub>2</sub> on the biogeochemistry of shallow marine sediments, their pore waters, and the  
45 646 overlying water column. *Int J Greenh Gas Control* In Press.  
46  
47  
48  
49  
50  
51  
52  
53  
54  
55  
56  
57  
58  
59  
60

- 1  
2  
3 647 Mantoura RFC & Woodward EMS (1983) Optimization of the indophenol blue method for the  
4 648 automated determination of ammonia in estuarine waters. *Estuar Coast Shelf Sci* 17: 219–  
5 649 224.  
6  
7  
8 650 Mehrbach C, Culbertson CH, Hawley JE & Pytkowicz RM (1973) Measurements of the apparent  
9 651 dissociation constants of carbonic acid in seawater at atmospheric pressure. *Limnol*  
10 652 *Oceanogr* 18: 897–907.  
11  
12 653 Metz B, Davidson O, De Coninck H, Loos M & Meyer L (2005) IPCC special report on carbon dioxide  
13 654 capture and storage. Intergovernmental Panel on Climate Change, Geneva (Switzerland).  
14 655 Working Group III.  
15  
16  
17 656 Middleburg JJ, Barranguet C, Boschker HT, Herman PM, Moens T & Heip CH (2000) The fate of  
18 657 intertidal microphytobenthos carbon: An in situ <sup>13</sup>C-labeling study. *Limnol Oceanogr* 45:  
19 658 1224-1234.  
20  
21  
22 659 Miller DC, Geider RJ & MacIntyre HL (1996) Microphytobenthos: the ecological role of the “secret  
23 660 garden” of unvegetated, shallow-water marine habitats. II. Role in sediment stability and  
24 661 shallow-water food webs. *Estuar Coast* 19: 202-212.  
25  
26  
27 662 Mohamed NM, Saito K, Tal Y & Hill RT (2010) Diversity of aerobic and anaerobic ammonia-oxidizing  
28 663 bacteria in marine sponges. *ISME J* 4: 38–48.  
29  
30  
31 664 Nübel U, Garcia-Pichel F & Muyzer G (1997) PCR primers to amplify 16S rRNA genes from  
32 665 cyanobacteria. *Appl Environ Microbiol* 63: 3327-32.  
33  
34 666 Paterson DM & Hagerthey SE (2001) Microphytobenthos in contrasting coastal ecosystems: biology  
35 667 and dynamics. In Reise K (eds) Ecological comparisons of sedimentary shores. Ecological  
36 668 studies vol. 151. Springer Verlag p 105-125.  
37  
38  
39 669 Pierrot D, Lewis E & Wallace DWR (2006) CO2sys DOS program developed for CO<sub>2</sub> system  
40 670 calculations. ORNL/CDIAC-105. Carbon Dioxide Information Analysis Centre, Oak Ridge  
41 671 National Laboratory, U.S. Department of Energy, Oak Ridge, Tennessee.  
42  
43  
44 672 Pruesse E, Quast C, Knittel K, Fuchs BM, Ludwig W, Peplies J & Glöckner FO (2007) SILVA: a  
45 673 comprehensive online resource for quality checked and aligned ribosomal RNA sequence  
46 674 data compatible with ARB. *Nucl Acids Res* 35: 7188-7196.  
47  
48  
49 675 Quince C, Lanzen A, Davenport RJ & Turnbaugh PJ (2011) Removing noise from pyrosequenced  
50 676 amplicons. *BMC bioinformatics* 12: 38.  
51  
52 677 Ramanan R, Kannan K, Deshkar A, Yadav R & Chakrabarti T (2010) Enhanced algal CO<sub>2</sub> sequestration  
53 678 through calcite deposition by *Chlorella* sp. and *Spirulina platensis* in a mini-raceway pond.  
54 679 *Bioresour Technol* 101: 2616-2622.  
55  
56  
57  
58  
59  
60

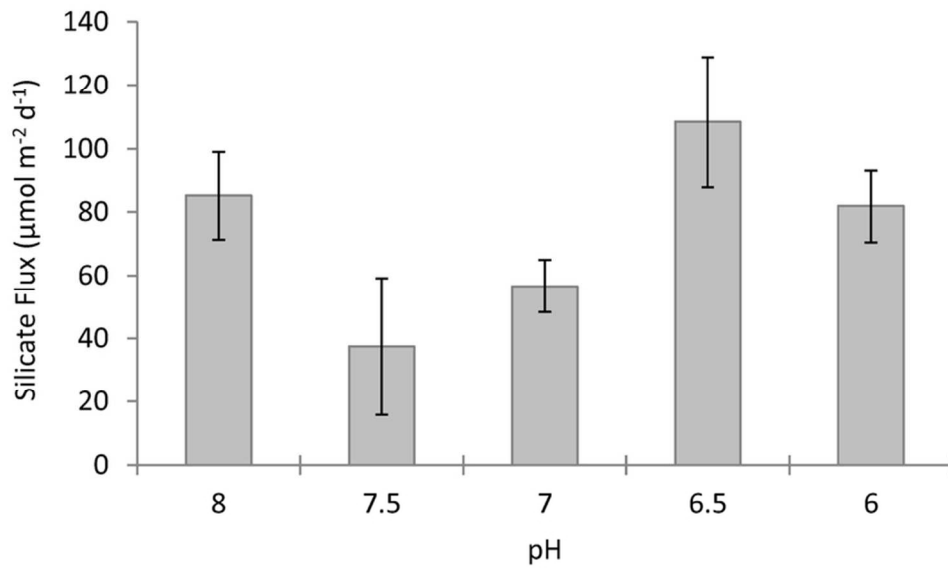
- 1  
2  
3 680 Rappe MS, Kemp PF & Giovannoni SJ (1997) Phylogenetic diversity of marine coastal picoplankton  
4 681 16S rRNA genes cloned from the continental shelf off Cape Hatteras, North Carolina. *Limnol*  
5 682 *Oceanogr* 42: 811-826.  
6  
7 683 Raven JA (1991) Physiology of inorganic C acquisition and implications for resource use efficiency by  
8 684 marine phytoplankton: relation to increased CO<sub>2</sub> and temperature. *Plant Cell Environ* 14:  
9 685 779–794.  
10  
11 686 Reinfelder JR (2011) Carbon concentrating mechanisms in Eukaryotic marine phytoplankton. *Annu*  
12 687 *Rev Mar Sci* 3:291–315.  
13  
14 688 Rost B, Riebesell U, Burkhardt S & Sültemeyer D (2003) Carbon acquisition of bloom forming marine  
15 689 phytoplankton. *Limnol Oceanogr* 48: 55–67.  
16  
17 690 Russell BD, Connell SD, Findlay HS, Tait K, Widdicombe S & Mieszkowska N. (2013) Ocean  
18 691 acidification and rising temperatures may increase biofilm primary productivity but decrease  
19 692 grazer consumption. *Philos T R Soc B*. 368(1627): 20120438.  
20  
21 693 Smith CJ, Nedwell DB, Dong LF & Osborn AM (2006) Evaluation of quantitative polymerase chain  
22 694 reaction-based approaches for determining gene copy and gene transcript numbers in  
23 695 environmental samples. *Environ Microbiol* 8: 804-815.  
24  
25 696 Stump M, Trübenbach K, Brennecke D, Hu MY & Melzner F (2012) Resource allocation and  
26 697 extracellular acid-base status in the sea urchin *Strongylocentrotus droebachiensis* in  
27 698 response to CO<sub>2</sub> induced seawater acidification. *Aqu Toxicol* 110-111: 194-207.  
28  
29 699 Sun J, Hutchins DA, Feng Y, Seubert EL, Caron DA & Fu FX (2011) Effects of changing pCO<sub>2</sub> and  
30 700 phosphate availability on domoic acid production and physiology of the marine harmful  
31 701 bloom diatom *Pseudo-nitzschia* multi-series. *Limnol Oceanogr* 56: 829-840.  
32  
33 702 Tait K, Laverock B, Shaw J, Somerfield PJ & Widdicombe S (2013) Minor impact of ocean acidification  
34 703 to the structure of the active microbial community in an Arctic sediment. *Env Microbiol Rep*  
35 704 5, 851-860.  
36  
37 705 Tait K, Stahl S, Taylor P & Widdicombe S (2015) Rapid response of the active microbial community to  
38 706 CO<sub>2</sub> exposure from a controlled sub-seabed CO<sub>2</sub> leak in Ardmucknish Bay (Oban, Scotland).  
39 707 *Int J Greenh Gas Control* In Press.  
40  
41 708 Tamura K, Dudley J, Nei M & Kumar S (2007) MEGA4: Molecular Evolutionary Genetics Analysis  
42 709 (MEGA) software version 4.0. *Mol Biol Evol* 24:1596-1599.  
43  
44 710 Taylor JD, Ellis R, Milazzo M, Hall-Spencer JM & Cunliffe (2014) Intertidal epilithic bacteria diversity  
45 711 changes along a naturally occurring carbon dioxide and pH gradient. *FEMS Microbiol Ecol* 89:  
46 712 670-678.  
47  
48  
49  
50  
51  
52  
53  
54  
55  
56  
57  
58  
59  
60

- 1  
2  
3 713 Taylor P, Stahl H, Blackford J, Vardy ME, Bull JM, Akhurst M, Hauton C, James RH, Lichtschlag A, Long  
4 714 D, Aleynik D, Toberman M, Naylor M, Connelly D, Smith D, Sayer DJ, Widdicombe S & Wright  
5 715 IC (2015a) Introduction to a novel in situ sub-seabed CO<sub>2</sub> release experiment for quantifying  
6 716 and monitoring potential ecosystem impacts from geological carbon storage. *Int J Greenh*  
7 717 *Gas Control* In Press.
- 8  
9  
10  
11 718 Taylor P, Lichtschlag A, Toberman M, Sayer MDJ, Reynolds A, Sato T & Stahl H (2015b) Impact and  
12 719 recovery of pH in marine sediments subject to a temporary carbon dioxide leak. *Int J Greenh*  
13 720 *Gas Control* In Press.
- 14  
15  
16 721 Thomsen J, Casties I, Pansch C, Körtzinger A & Melzner F. (2013) Food availability outweighs ocean  
17 722 acidification effects in juvenile *Mytilus edulis*: laboratory and field experiments. *Global*  
18 723 *Change Biology* 19: 1017–1027.
- 19  
20  
21 724 Torstensson A, Chierici M & Wulff A (2012) The influence of increased temperature and carbon  
22 725 dioxide levels on the benthic/sea ice diatom *Navicula directa*. *Polar Biol* 35: 205-214.
- 23  
24 726 Tortell PD, Payne CD, Li YH, Trimborn S, Rost B, Smith WO, Riesselman C, Dunbar RB, Sedwick P &  
25 727 DiTullio GR (2008) CO<sub>2</sub> sensitivity of Southern Ocean phytoplankton. *Geophys Res Lett* 35,  
26 728 L04605, doi:10.1029/2007GL032583.
- 27  
28  
29 729 Trimborn S, Wolf-Gladrow D, Richter KU & Rost B (2009). The effect of pCO<sub>2</sub> on carbon acquisition  
30 730 and intracellular assimilation in four marine diatoms. *J Exp Mar Biol Ecol* 376: 26-36.
- 31  
32 731 Underwood GJC & Kromkamp J (1999) Primary production by phytoplankton and  
33 732 microphytobenthos in estuaries. *Adv Ecol Res* 29: 93-153.
- 34  
35 733 Widdicombe S & Needham HR (2007) Impact of CO<sub>2</sub>-induced seawater acidification on the  
36 734 burrowing activity of *Nereis virens* and sediment nutrient flux. *Mar Ecol Prog Ser* 341: 111–  
37 735 122.
- 38  
39  
40 736 Yanagawa K, Morono Y, de Beer D, Haeckel M, Sunamura M, Futagami T, Hoshino T, Terada T,  
41 737 Nakamura K, Urabe T, Rehder G, Boetius A & Inagaki F (2012) Metabolically active microbial  
42 738 communities in marine sediment under high-CO<sub>2</sub> and low-pH extremes. *ISME J* 7: 555-567.
- 43  
44  
45 739 Zhang JZ & Chi J (2002) Automated analysis of nanomolar concentrations of phosphate in natural  
46 740 waters with liquid waveguide. *Environ Sci Technol* 36: 1048–1053.

**Table 1:** Environmental conditions in the cores averaged over the 10 week experimental period, values are means ( $\pm$  95 % confidence intervals). pH, temperature ( $^{\circ}$ C), salinity and total alkalinity (TA,  $\mu\text{mol kg}^{-1}$ ) were measured and used to calculate  $\text{pCO}_2$  ( $\mu\text{atm}$ ), dissolved inorganic carbon (DIC,  $\mu\text{mol kg}^{-1}$ ), and saturation states for calcite ( $\Omega_{\text{c}}$ ) and aragonite ( $\Omega_{\text{A}}$ ). Also shown are average water nutrient concentrations ( $\mu\text{M}$ ) calculated from measurements taken throughout the 10 week incubation period.

target pH	8.0	7.5	7.0	6.5	6.0
pH	7.98 ( $\pm$ 0.021)	7.47 ( $\pm$ 0.043)	7.11 ( $\pm$ 0.032)	6.69 ( $\pm$ 0.032)	6.14 ( $\pm$ 0.030)
Temperature ( $^{\circ}$ C)	10.8 ( $\pm$ 0.08)	11.0 ( $\pm$ 0.12)	11.1 ( $\pm$ 0.14)	10.8 ( $\pm$ 0.07)	10.6 ( $\pm$ 0.09)
Salinity	33.8 ( $\pm$ 0.10)	33.7 ( $\pm$ 0.08)	33.7 ( $\pm$ 0.07)	33.8 ( $\pm$ 0.08)	33.7 ( $\pm$ 0.07)
TA ( $\mu\text{mol kg}^{-1}$ )	2561 ( $\pm$ 50)	2512 ( $\pm$ 49)	2531 ( $\pm$ 53)	2572 ( $\pm$ 39)	2594 ( $\pm$ 83)
$\text{pCO}_2$ ( $\mu\text{atm}$ )	711 ( $\pm$ 25)	2382 ( $\pm$ 190)	5627 ( $\pm$ 309)	15157 ( $\pm$ 924)	54396 ( $\pm$ 1902)
DIC ( $\mu\text{mol kg}^{-1}$ )	2441 ( $\pm$ 40)	2564 ( $\pm$ 35)	2748 ( $\pm$ 38)	3214 ( $\pm$ 30)	4937 ( $\pm$ 52)
$\Omega_{\text{c}}$	2.52 ( $\pm$ 0.16)	0.84 ( $\pm$ 0.10)	0.37 ( $\pm$ 0.04)	0.14 ( $\pm$ 0.02)	0.04 ( $\pm$ 0.01)
$\Omega_{\text{A}}$	1.6 ( $\pm$ 0.11)	0.53 ( $\pm$ 0.07)	0.24 ( $\pm$ 0.02)	0.09 ( $\pm$ 0.01)	0.03 ( $\pm$ 0.01)
Ammonia	0.85 ( $\pm$ 0.33)	0.75 ( $\pm$ 0.27)	0.55 ( $\pm$ 0.13)	0.70 ( $\pm$ 0.4)	0.85 ( $\pm$ 0.21)
Nitrate	6.15 ( $\pm$ 1.01)	6.51 ( $\pm$ 1.18)	6.93 ( $\pm$ 0.94)	5.96 ( $\pm$ 0.97)	6.33 ( $\pm$ 0.93)
Nitrite	0.14 ( $\pm$ 0.018)	0.14 ( $\pm$ 0.021)	0.13 ( $\pm$ 0.019)	0.10 ( $\pm$ 0.013)	0.15 ( $\pm$ 0.027)
Phosphate	0.55 ( $\pm$ 0.09)	0.64 ( $\pm$ 0.16)	0.63 ( $\pm$ 0.12)	0.68 ( $\pm$ 0.11)	0.69 ( $\pm$ 0.11)
Silicate	5.25 ( $\pm$ 0.41)	5.20 ( $\pm$ 0.54)	5.13 ( $\pm$ 0.38)	5.38 ( $\pm$ 0.44)	5.27 ( $\pm$ 0.42)

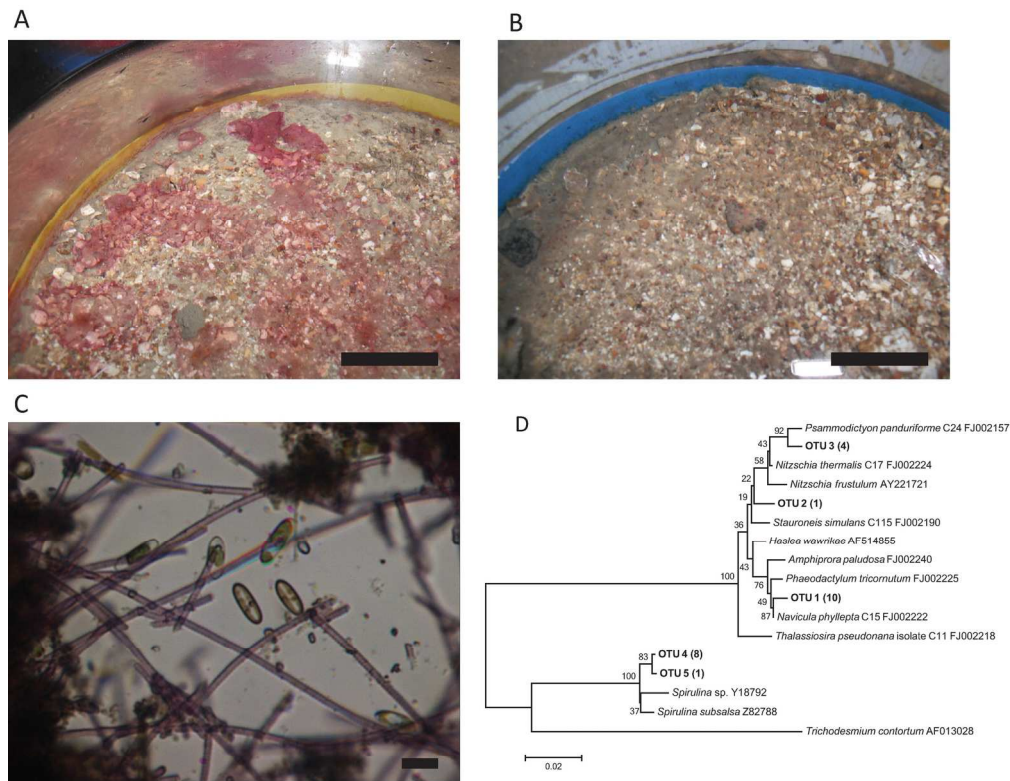
1  
2  
3  
4  
5  
6  
7  
8  
9  
10  
11  
12  
13  
14  
15  
16  
17  
18  
19  
20  
21  
22  
23  
24  
25  
26  
27  
28  
29  
30  
31  
32  
33  
34  
35  
36  
37  
38  
39  
40  
41  
42  
43  
44  
45  
46  
47  
48  
49  
50  
51  
52  
53  
54  
55  
56  
57  
58  
59  
60



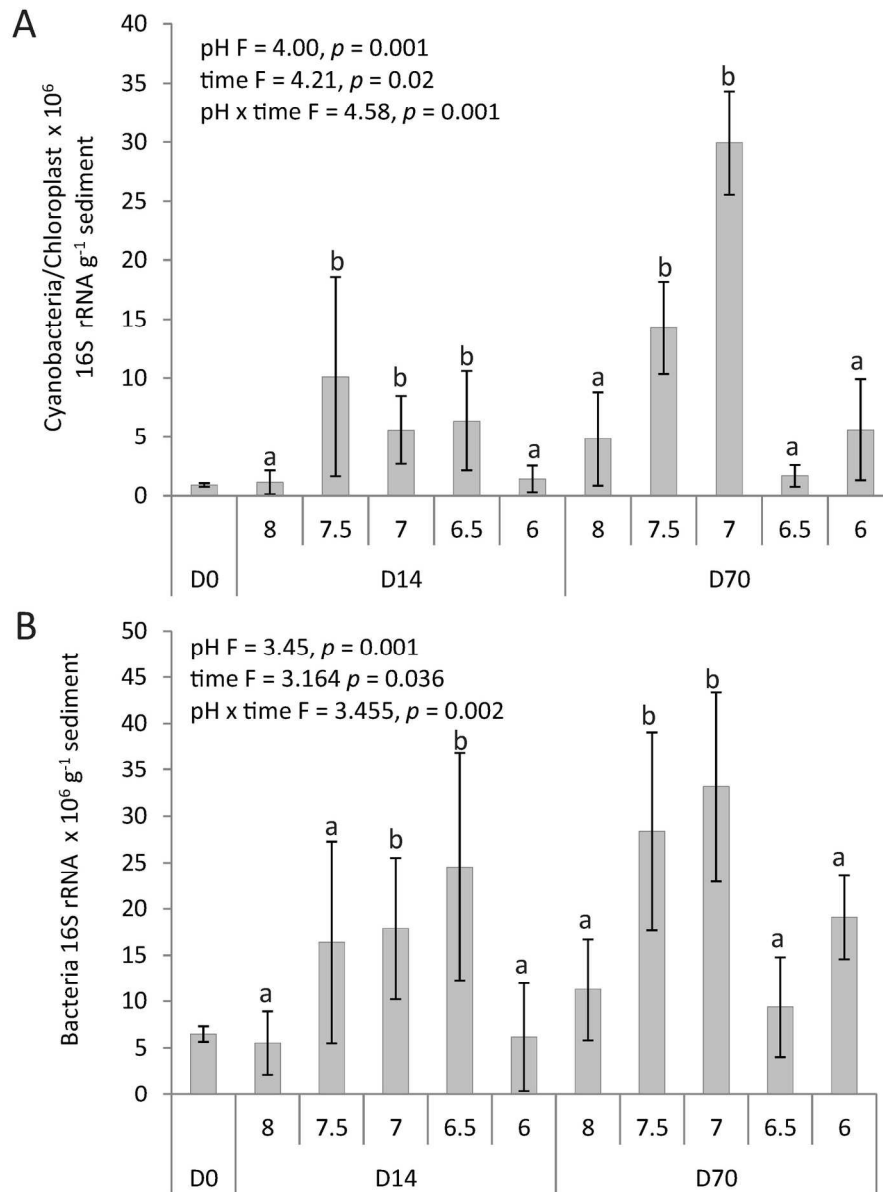
Impact of seawater pH on average silicate flux rates. Error bars are standard deviation (n = 5).  
76x45mm (300 x 300 DPI)

Peer Review

1  
2  
3  
4  
5  
6  
7  
8  
9  
10  
11  
12  
13  
14  
15  
16  
17  
18  
19  
20  
21  
22  
23  
24  
25  
26  
27  
28  
29  
30  
31  
32  
33  
34  
35  
36  
37  
38  
39  
40  
41  
42  
43  
44  
45  
46  
47  
48  
49  
50  
51  
52  
53  
54  
55  
56  
57  
58  
59  
60

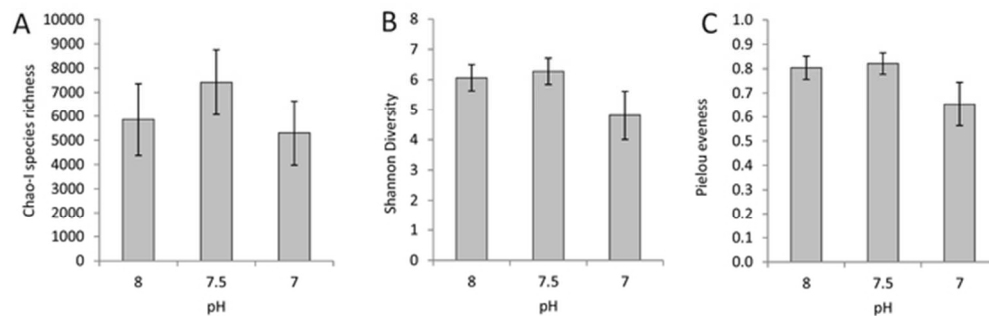


Comparison of sediment surface of cores incubated at pH 7.0 (A) and pH 8.0 (B). A pink mat of microphytobenthos mat can be clearly seen in the cores exposed to pH 7.0. Bar is 3 cm. (C) Microscope image of microphytobenthos mat showing the presence of pink cyanobacterial filaments and diatoms. Bar is 100 μm. (D) Phylogenetic tree of Cyanobacterial and Chloroplast 16S rRNA OTU data derived from clone libraries of segments of the pink microphytobenthos mat calculated using MEGA 5 (Tamura et al., 2007). OTUs were identified at 97% nucleotide similarity. The number of sequences found within each OTU is indicated in brackets. The tree topology is based on maximum likelihood and bootstrap analysis was performed with 1000 replications (MEGA 5). Reference sequences and their accession numbers are also shown  
171x165mm (300 x 300 DPI)

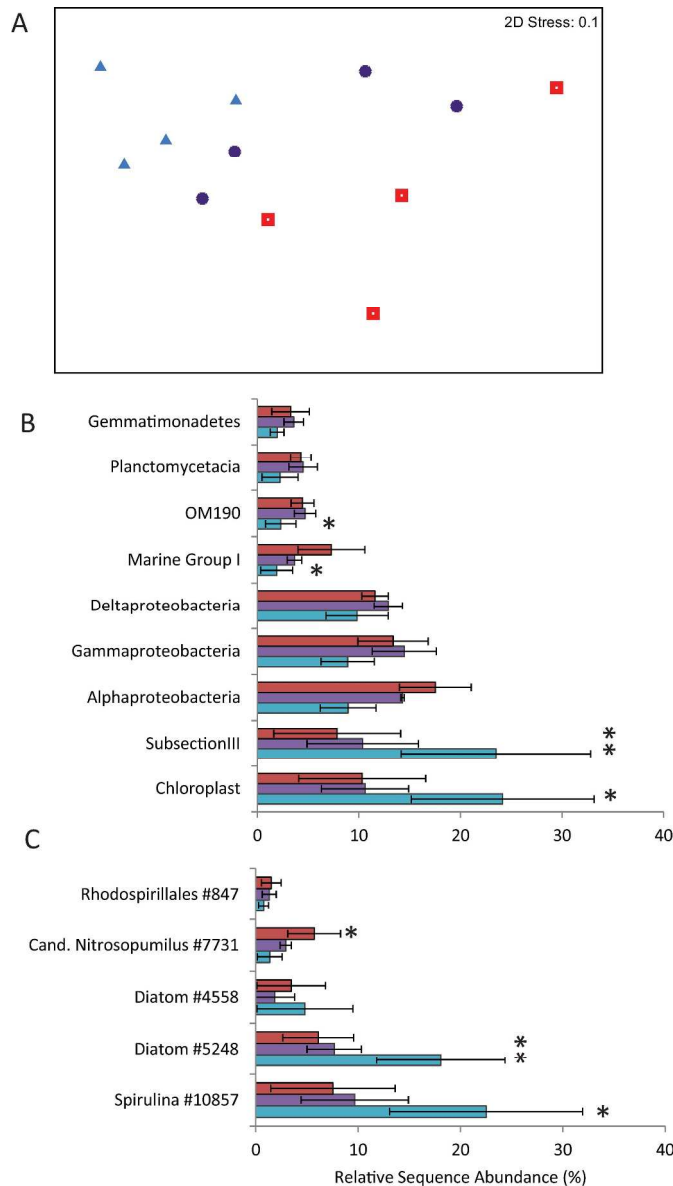


Effect of pH on the abundance of cyanobacterial/micro-algal 16S rRNA (g<sup>-1</sup> sediment). For each pH, five separate cores were used. The results of PEMAANOVA tests for significant difference between pH treatments and week sampled are shown above each graph. Statistical differences between all treatments are indicated by asterisks: \*\*\* $p \leq 0.001$ , \*\* $p \leq 0.01$ , \* $p \leq 0.05$ ; significant differences ( $p \leq 0.05$ ) between individual treatments are indicated by different letters. Error bars are standard deviation ( $n = 5$ ).

158x208mm (300 x 300 DPI)



Effect of pH on measurements of alpha diversity including (A) Chao-I species richness, (B) Shannon diversity and (C) Pielou evenness. Error bars are standard deviation (n = 5).  
57x18mm (300 x 300 DPI)



The effect of pH on microbial community composition including (A) Non-metric multidimensional scaling (MDS) ordination of a Bray–Curtis resemblance matrix (red open squares are pH 8.0, purple asterisks are pH 7.5 and blue closed triangles pH 7.0), and the effect of pH on (A) the abundance of the microbial classes with abundances > than 2%, and (B) the top five most abundant OTUs. Blue bars are pH 7.0, purple bars are pH 7.5 and red bars are pH 8.0 treatments. Significant differences when compared to pH 8.0 treatments at each time point are indicated by \*\* for  $p \leq 0.01$  and \* for  $p \leq 0.05$ . Error bars are standard deviation ( $n = 5$ ).

229x403mm (300 x 300 DPI)

**Supplementary Table 1:** Comparison of sequence data from each core and CO<sub>2</sub> treatment. Shown are the number of sequences per sample post-processing, the number of OTUs (clustered at 97% sequence similarity) and the ratio of bacterial:archaeal sequences in the data-set. This is compared to the ratio of bacteria:archaea obtained by RT qPCR of 16S rRNA. Due to the variability amongst the numbers of sequences obtained for each sample, all cores were sub-sampled to the lowest value, 5237 (obtained for core no. 28). Also shown (in bold) are totals calculated from combined sequence data from each CO<sub>2</sub> treatment.

pH	Core Number	RAW DATA			Ratio Archaea: Bacteria qPCR	RE-SAMPLED DATA (5237 sequences per core) - 97% similarity	
		No. sequences	No. OTUs	Ratio Archaeal: Bacterial sequences		No. OTUs	Ratio Archaeal: Bacterial sequences
8	26	7490	3482	0.05	0.04	1916	0.05
	27	7002	2794	0.11	0.11	1686	0.11
	28	5237	2664	0.07	0.08	1861	0.07
	29	8843	4629	0.12	0.18	2118	0.13
	<b>TOTAL</b>	<b>28572</b>	<b>13406</b>	<b>0.09</b>	<b>0.10</b>	<b>5630</b>	<b>0.09</b>
7.5	31	9869	4205	0.03	0.03	1963	0.03
	32	10292	4025	0.04	0.09	1789	0.05
	33	10109	5143	0.07	0.09	2307	0.07
	35	11535	6257	0.04	0.07	2288	0.04
	<b>TOTAL</b>	<b>41805</b>	<b>19403</b>	<b>0.05</b>	<b>0.07</b>	<b>6442</b>	<b>0.05</b>
7	37	10712	4594	0.01	0.04	2052	0.01
	38	6870	2312	0.10	0.08	1395	0.10
	39	6199	1943	0.03	0.05	1335	0.03
	40	15424	4425	0.01	0.04	1485	0.01
	<b>TOTAL</b>	<b>39205</b>	<b>13162</b>	<b>0.04</b>	<b>0.05</b>	<b>4931</b>	<b>0.04</b>